04,05

Cyclotron resonance in YFe_5O_{12} single crystals

© E.I. Golovenchits, V.A. Sanina ¶, B.Kh. Khannanov, M.P. Shcheglov

Ioffe Institute,
St. Petersburg, Russia

¶ E-mail: sanina@mail.ioffe.ru

Received November 12, 2024
Revised November 20, 2024
Accepted November 22, 2024

Cyclotron resonance is found in nanosized local regions single crystal samples of yttrium-iron garnet. This resonance was observed in 8 mm microwave range at room temperature. This resonance manifests itself as in the form of free- electrons subsystem excitations, or in the form of mixed spin-electron modes. The existence of cyclotron resonance convincingly indicates the presence phenomenon of Phase Separation in yttrium-iron garnet single crystals.

Keywords: Electron resonance, phase separation regions, domain walls.

DOI: 10.61011/PSS.2024.11.60088.303

1. Introduction

We observed phase separation regions (PSR) while studying magnetic dynamics in yttrium iron garnets (YIG) [1,2]. Previously, PSR were observed only in crystals with magnetic ions that have variable valence or in crystals containing impurities that cause a change in the valence of magnetic ions. A mechanism was proposed in [2,3], firstly introduced in [3], that assumes that in magnetic crystals with a domain structure, at the boundaries between 180-degree magnetic domains, in the Neel-type domain walls, structural distortions occur that breaks the central symmetry. This results in the formation of a local electric field in the domain walls, leading to the accumulation of electrons within them. Ferromagnetically polarized electrons contribute to the double exchange process and the formation of PSR containing free and polarized charge carriers.

The purpose of this study was to detect cyclotron resonance (CR) on charge carriers localized in the phase separation regions [1].

2. Theory

YIG single crystals have cubic symmetry (O_h^{10}). Fe^{3+} ions occupy two different positions: three ions are in the oxygen tetrahedron, and two ions are in the oxygen octahedron. Nonmagnetic Y^{3+} ions are located in oxygen dodecahedrons. The spins of Fe^{3+} ions in different positions in the crystal have opposite orientations, forming a magnetic structure with a difference magnetic moment with a Neel temperature $T_N = 560$ K (ferrimagnetic state). YIG shows itself as a good dielectric at low frequencies. No significant broadening of the ferromagnetic resonance (FMR) lines was observed at frequencies of the order of 30 GHz, at which measurements were performed in this study, i. e. the dielectric state of the main volume of the crystal does not change, and delocalized carriers exist only in regions of small volume, i. e. in phase separation regions.

CR is a type of magnetic resonance that occurs when free charge carriers absorb electromagnetic energy in the presence of a magnetic field. The existence of CR as a special type of magnetic resonance, which differs from resonances of a spin nature, was considered in theoretical works [4–7] and it was later confirmed experimentally [8,9]. The basic principles of CR have been discussed in detail in several monographs and review articles [10,11].

Free charged particles move in an applied permanent magnetic field H in a spiral with its axis directed along the field. In this case, electrons form coils in a plane perpendicular to the $\boldsymbol{H}$, i. e. the motion in that plane is finite and periodic. This situation is subject to quantization, and the solution to the Schrödinger equation results in a discrete set of states with constant energy described by the quantum number, n (Landau levels). Thus, the continuous spectrum of electrons without a magnetic field becomes discrete in the presence of the H

$$\varepsilon_n = \frac{e\hbar}{mc} H\left(n + \frac{1}{2}\right), \tag{1}$$

where ε_n is the energy of the nth level, e is the charge, m is the mass of the electron, $\hbar$ is Planck's constant, c is the speed of light.

The Landau levels have a finite width

$$\varepsilon_n = \frac{e\hbar}{mc} H. \tag{2}$$

Each level is degenerate, and the splitting of states within levels is determined by the quantum number l:

$$\varepsilon_{nl} = \frac{e\hbar}{mc} H\left(n + l + \frac{1}{2}\right). \tag{3}$$

From a classical point of view, the quantization of an electron's energy in a magnetic field corresponds to the quantization of its orbital radius. Cyclotron resonance is the transition between adjacent n and $n+1$ states, induced by an alternating electric field. Accordingly, the frequency of CR is determined by expression

$$w_c = \frac{e}{mc} H. \tag{4}$$

The CR frequency for a free electron gas coincides with the spin resonance frequency (EPR, FMR for a g-factor is equal to 2 and there is no anisotropy). However, its nature is different. If spin resonances are based on magnetic dipole transitions, which are excited by the magnetic component $h^{\sim}$ of the alternating field, perpendicular to the field $\boldsymbol{H}$, then CR is an electric dipole transition and is excited by the electric component $\varepsilon^{\sim}$, perpendicular to the field $\boldsymbol{H}$. The intensity of electric dipole transitions is much greater than the intensity of magnetic dipole transitions. Therefore, a significantly lower concentration of electrons is required to observe CR. This is used when studying CR in solids, because a low concentration reduces the probability of electron scattering and allows for the conditions necessary to observe CR to be realized. The basic equations for CR in a free electron gas still apply to free carriers in solids, but the values for mass (m) and momentum (k) are replaced with effective parameters — the cyclotron mass (m_c) and quasi-momentum $(k^{\sim})$. These effective parameters depend on the crystal's properties, such as the type and shape of its Fermi surface, which determine its kinetic characteristics. For low-symmetry crystals with complex Fermi surfaces, the effective mass is a tensor. In the case of cubic crystals with a simple spherical Fermi surface, this is a scalar quantity, but its magnitude may differ from m. In order for CR to exist, the relaxation time of the electrons during precession must be long enough for several rotations to be performed without scattering. Collisions between electrons and phonons in the crystal lattice are the main sources of scattering in non-magnetic crystals. Spin-spin and spin-lattice relaxation mechanisms are usually less significant. Such concentration of charge carriers can be achieved in semiconductor crystals due to a decrease of temperature that makes both main mechanisms of electronic relaxation quite small.

Recently, low-dimensional structures — quantum wells — have been extensively studied. Polarization barriers at the boundaries in these structures effectively isolate the inner volume of the well from the rest of the crystal lattice. The mean free path of electrons can significantly increase in these quantum wells, making it possible to observe quantum effects even at high temperatures [12]. However, there is an additional limitation for CR in quantum wells. The frequency at which CR can occur must be higher than a minimum value, which depends on the size of the quantum well in the direction perpendicular to the magnetic field, i. e., the plane of the electron orbits at CR. This minimum frequency is determined by the condition that the radius of the cyclotron orbit (r_c) must be smaller than the size of the well (Lt).

$$r_c = \frac{m_c c}{eH} V_F. \tag{5}$$

here, V_F is the velocity of electrons on the Fermi surface:

$$V_F = \frac{\hbar k_F}{m_c} = \frac{\hbar}{m_c} \sqrt[3]{\frac{3\pi^2 N}{v}}, \tag{6}$$

k_F is the momentum of electrons on the Fermi surface, N is the concentration of electrons on the Fermi surface, v is its volume. Phase separation regions are a variant of a quantum well, and polarization barriers at their boundaries can provide conditions for the existence of CR at high temperatures.

From the point of view of observing CR, the main feature of YIG and other ferromagnetically ordered crystals compared to non-magnetic semiconductors is the presence of intense, homogeneous (FMR), and inhomogeneous magnetic system excitations, which can strongly influence delocalized electron excitations (CR). It is necessary to create conditions where spin and electronic vibrations weakly influence each other for identifying CR features that distinguish it from magnetic system spin excitations in a crystal. This is taken into account in the experimental methodology developed in this work.

3. Materials and methods

We will assume that, the Fermi surface has a simple shape of a spheroid or an ellipsoid in YIG, as in many other cubic crystals that is elongated along its major axis. The samples were oriented so that when measuring the CR, the $\langle 111 \rangle$ axis of the crystal was directed along the magnetic field, $\boldsymbol{H}$. We used YIG single crystal samples in the form of spheres with a diameter of approximately 0.5 mm. The main characteristics of the samples are provided in Table.

In the table: ΔH is the FMR linewidth measured at 30 GHz, ω is the half-width of the swing curves, orientation of samples: direction $\langle 111 \rangle$ along the normal, reflex 444, $\Theta_B = 26°$. The observed scatter of ω values in case of rotation around the $\langle 111 \rangle$ axis indicates some blockiness of the structure.

The measurements were carried out using a magnetic resonance spectrometer in the 8 mm microwave range, using a per-pass scheme. The dependences of the transmission coefficient through the measuring cell with the sample on the magnetic field were measured. A magnetic field H with a range of 0−16 kOe was applied at a speed of 2 Oe/sec. A TE_{10n} fundamental mode resonator, made from a standard waveguide with a cross section of 7.2×3.4 mm, was used as the measuring cell. A sample on a quartz holder was placed in the center of the resonator.

Main characteristics of the samples

N	∅, mm	ΔH, Oe	ω (half-width)
1	0.6	15	15–30′
2	0.55	6	14–40′
3	0.52	1 – 2	30′

4. Results and discussion

When the fundamental mode is excited in the resonator, depending on the frequency, the sample finds itself either at the antinode of the electric field ($\varepsilon^{\sim}$ for n — odd) or at the magnetic field ($h^{\sim}$ for n — even), where n is the number of half-waves that fit along the length of the resonator. When measuring CR, the frequency corresponding to odd n is used, and when measuring FMR, the frequency corresponding to even n is used. In the case of CR, the resonator is rotated around the horizontal axis so that the long wall of the cross-section is aligned with the field $\boldsymbol{H}$ (configuration C). When measuring FMR the resonator is installed with the long wall perpendicular to $\boldsymbol{H}$ (configuration F). The structure of the microwave field inside the resonator is shown in Figure 1.

The electric component of the microwave field, $\varepsilon^{\sim}$, has only a y-component. Its value along the x and z axes at a given location in the sample is determined by the following expression:

$$\varepsilon^{\sim} = \varepsilon_y = \varepsilon_0 \sin\frac{\pi x}{a} \sin\frac{\pi z n}{l}. \qquad (7)$$

a, L — the dimensions of the resonator along the x and z axes, respectively. Since the antinodes and nodes for the electric and magnetic components are shifted by $\lambda_g/4$ (λ_g is the wavelength in the resonator) and the polarizations of these components are orthogonal, it is important to ensure maximum possible isolation when measuring CR and FMR. However, in reality, it is necessary to take into account obvious limitations caused by the finite size of the samples, the inaccuracy in their installation, and limitations associated with the redistribution of the microwave field in the resonator with the sample in comparison with its distribution in an empty resonator. The presence of gyrotropy in the sample leads to different propagation constants for forward and backward waves in the resonator, making a single-mode state impossible and causing the emergence of higher modes that blur the positions of the antinodes and nodes of the main mode. In addition, when the FMR is excited, a secondary microwave wave is generated. The amplitude of this wave depends on the intensity of the resonance signal, which in turn depends on the width of the resonance curve ΔH, the magnitude of the magnetization of the sample, and its size. This field can exceed the field in the resonator without a sample. It also contains a component $\varepsilon^{\sim}$ that is capable of exciting the CR in configuration F [13–15]. Nonlinear effects may also occur with narrow and intense FMR lines in case of which a longitudinal component of the alternating magnetic moment appears during precession. The usual estimate for the threshold microwave field strength, starting from which nonlinear effects become significant, is $h_c \leq \Delta H/2$. Considering all these factors, we used samples with minimal sizes and different ΔH values (see table), and performed measurements at low microwave powers. At the same time, it was possible to establish a fairly weak coupling between FMR and CR in some cases. Figures 2, 3 and 4 show the results of measurements on samples in configurations C and F at microwave frequencies corresponding to the positions of the samples at antinode $\varepsilon^{\sim}$ or $h^{\sim}$. Red lines indicate the samples at the antinode $\varepsilon^{\sim}$, while samples at antinode $h^{\sim}$ are shown by black lines. The configurations and other experimental parameters for each sample are listed in the figure captions. All measurements presented in Figures 2, 3 and 4 were conducted at a constant level of microwave power incident (detector voltage $P_0 = 1$ mV). We estimated the power level based on the detector voltage, which allowed comparing the relative values of power for different measurements, but not the absolute value. The maximum power level of the microwave generator is 3 mW.

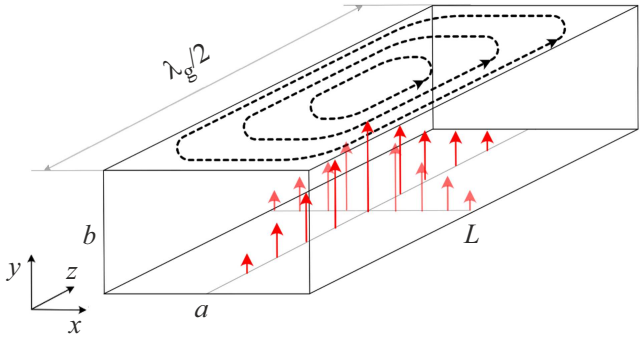

Figure 1. Structure of the microwave field in the resonator.

4.1. Results of measuring samples in the resonator

4.1.1. Results for sample N 1

Figure 2 shows the measurement results for sample N 1. A resonant signal is seen in configuration C in the electric field antinode at a field of $H \approx 11.2$ kOe close to the value of ω/γ (where ω is the resonant frequency and γ is gyromagnetic ratio) for a given frequency (Figure 2, *a*, red line). No resonance signals were not detected in the same configuration in the magnetic field antinode (Figure 2, *a*, black line) in the region of fields $H \approx 10.7$ kOe, corresponding to the frequency of ω/γ. The resonant signal in the antinode of the electric field is naturally associated with CR. Therefore, the connection between FMR and CR is weak for this sample in configuration C, and the observed behavior corresponds to

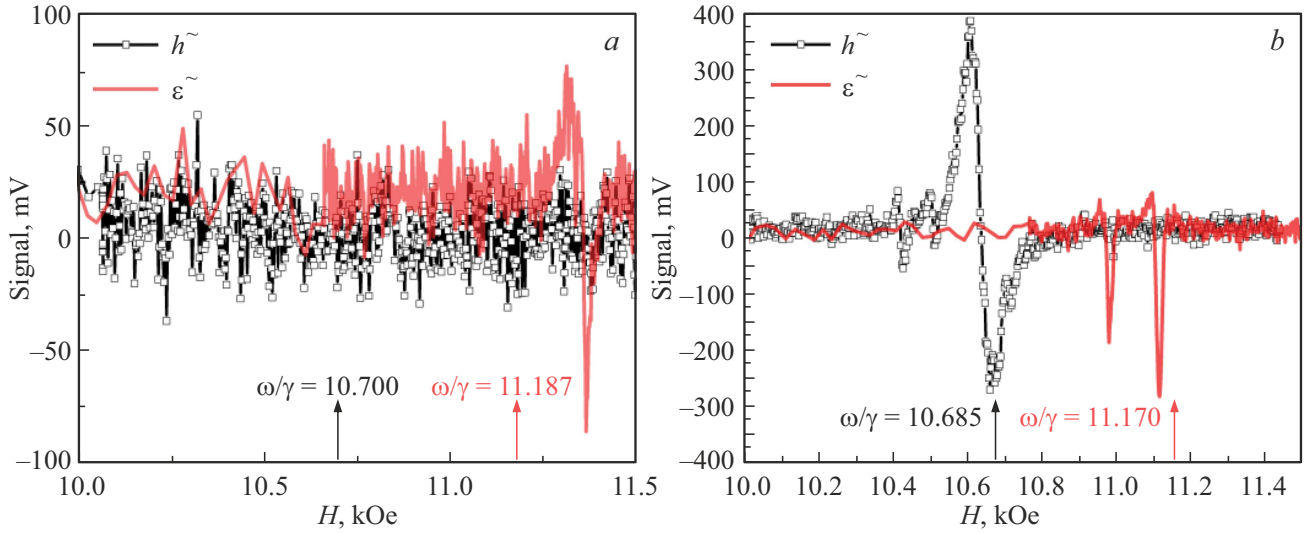

Figure 2. Results for sample N 1: *a*) configuration C, *b*) configuration F.

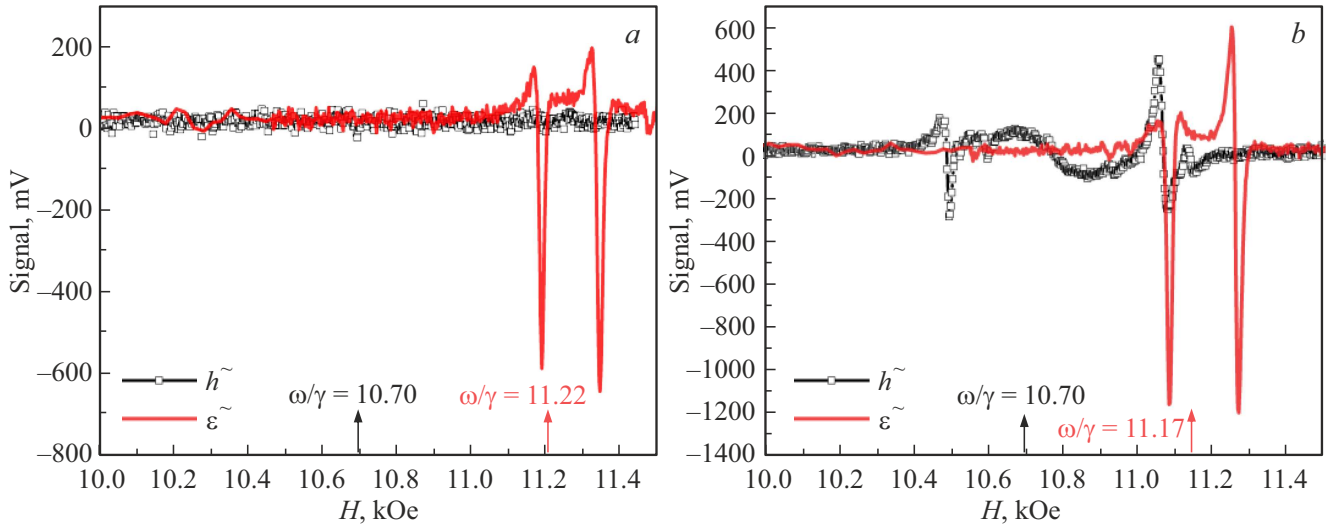

Figure 3. Results for sample N 2: *a*) configuration C, *b*) configuration F.

the accepted model. In configuration F (Figure 2, *b*), unlike the C configuration, FMR is polarisation resolved, and it is observed in the magnetic field antinode (Figure 2, *b*, black line) near $H \approx 10.7$ kOe corresponding to the value of ω/γ at this frequency. Several satellites, which may represent inhomogeneous precession types were visible together with the main line. Two intense signals are visible at the antinode of the electric field in this configuration (Figure 2, *b*, red line), which we believe to be CR signals. We assume that the presence of two signals is attributable to the splitting of states based on the quantum number l (see formulas (1) and (2)). The observed signals correspond to the CR of electrons occupying states split by quantum number l. This interpretation is supported by the small value of the splitting ($\delta\omega/\omega = 0.01-0.015$) and the dependence of the ratio of signal amplitudes on microwave power. We will discuss the dependence of signal amplitude on microwave power in more detail later, when we consider the results for sample N 3.

It is also possible that these signals correspond to both electron CR and hole CR, as the microwave wave in the resonator has a linear polarization, and its right-handed circular component excites electron CR, while its left-handed circular component excites hole CR. However, we find this explanation less likely.

4.1.2. Results for sample N 2

Figure 3 shows the measurement results for sample N 2, which has a slightly narrower FMR line than sample N 1.

The results are similar to those obtained for sample N 1, as can be seen. The signals are completely identical in

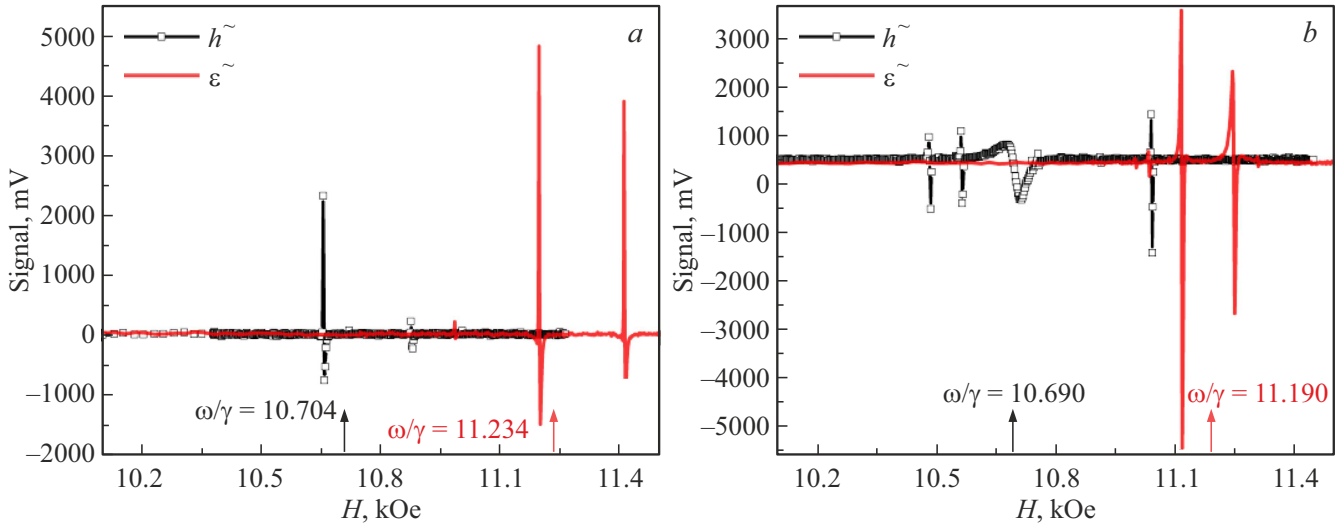

Figure 4. Results for sample N 3: *a*) configuration C, *b*) configuration F.

configuration C. There is no signal in the area of fields near $\omega/\gamma \approx 10.7$ kOe corresponding to FMR in configuration C, and there is a signal at $\omega/\gamma \approx 11.2$ kOe corresponding to CR although only one peak was observed unlike the sample N 1. FMR is clearly observed in the fields of $\omega/\gamma \approx 10.7$ kOe in the configuration F, and peaks corresponding to CR are visible at $\omega/\gamma \approx 11.2$ kOe. An additional peak is also visible in the F configuration, shifted from the area near $\omega/\gamma \approx 10.7$ kOe towards higher fields. It should be noted that while different samples are oriented the same way ($\langle 111 \rangle \parallel H$) in the configuration C, but they may have different orientations in the configuration F, since the samples were not oriented in the (111) plane.

4.1.3. Results for sample N 3

Let us now consider the results for sample N 3, which has the narrowest ($\Delta H \approx 1-2$ Oe) FMR line (Figure 4). There are two intense peaks in this sample in the C configuration at the electric field antinode near $H = \omega/\gamma \approx 11.2$ kOe, as in previous cases (Figure 4, *a*). We still classify these peaks as CR, but several weaker signals are also visible at the magnetic field antinode at $\omega/\gamma \approx 10.7$ kOe in this configuration compared to signals at $\varepsilon^{\sim}$ antinode, because when FMR is intense, a strong coupling occurs between CR and FMR. Signals are observed at the electric field antinodes in the F configuration, which differ little from those observed at the antinode $\varepsilon^{\sim}$ in C configuration. Numerous signals are found at the antinodal region of the magnetic fields which are difficult to interpret unambiguously without further research. In the case of a small ΔH, the coupling between magnetic and charge excitations is so strong that mixed modes occur, which are excited by both the electric and magnetic components of the microwave field, with slightly different efficiencies. To reduce this coupling, we measured the extremely low power of the exciting microwave field. Achieving this regime in a resonator is difficult, so these measurements were conducted in a waveguide.

4.2. Results of measurements in the waveguide

Figure 5 shows the results of these measurements. It can be seen that, resonance signals are not observed in configuration C, at $P_0 < 0.2$ mV. A resonant signal appears initially at $P_0 > 0.2$ mV, and then two signals of different intensities are observed at $P_0 > 1$ mV. The amplitudes of both observed signals become equal at high power levels ($P_0 \approx 100$ mV). There is no threshold for microwave field amplitude in configuration F (Figure 5, *d*), and a resonant signal is clearly visible at $P_0 \approx 0.13$. There are conditions for the excitation of both the CR and FMR in amplitude $\varepsilon^{\sim}$ and $h^{\sim}$ both in C and F configurations because a travelling wave mode is used in the waveguide. However, there is polarization decoupling, which is stronger than in a resonator, due to the lack of higher modes of waves. Thus the microwave threshold observed in configuration C should be attributed to CR. The existence of this threshold for CR is due to the fact that the delocalized electrons in PSR are not completely free. They are weakly bound at the charged boundaries of PSR and require a certain amount of electrical microwave field to release them.

The observed dependence on the CR microwave signal power agrees with the concept that these signals correspond to splitting in *l*. The existence of exactly two signals and the dependence of their amplitudes on microwave power may be due to some difference of CR frequencies for transitions with preservation and variation of the spin projection and the dependence of the probability of these transitions on the kinetic energy of the electrons.

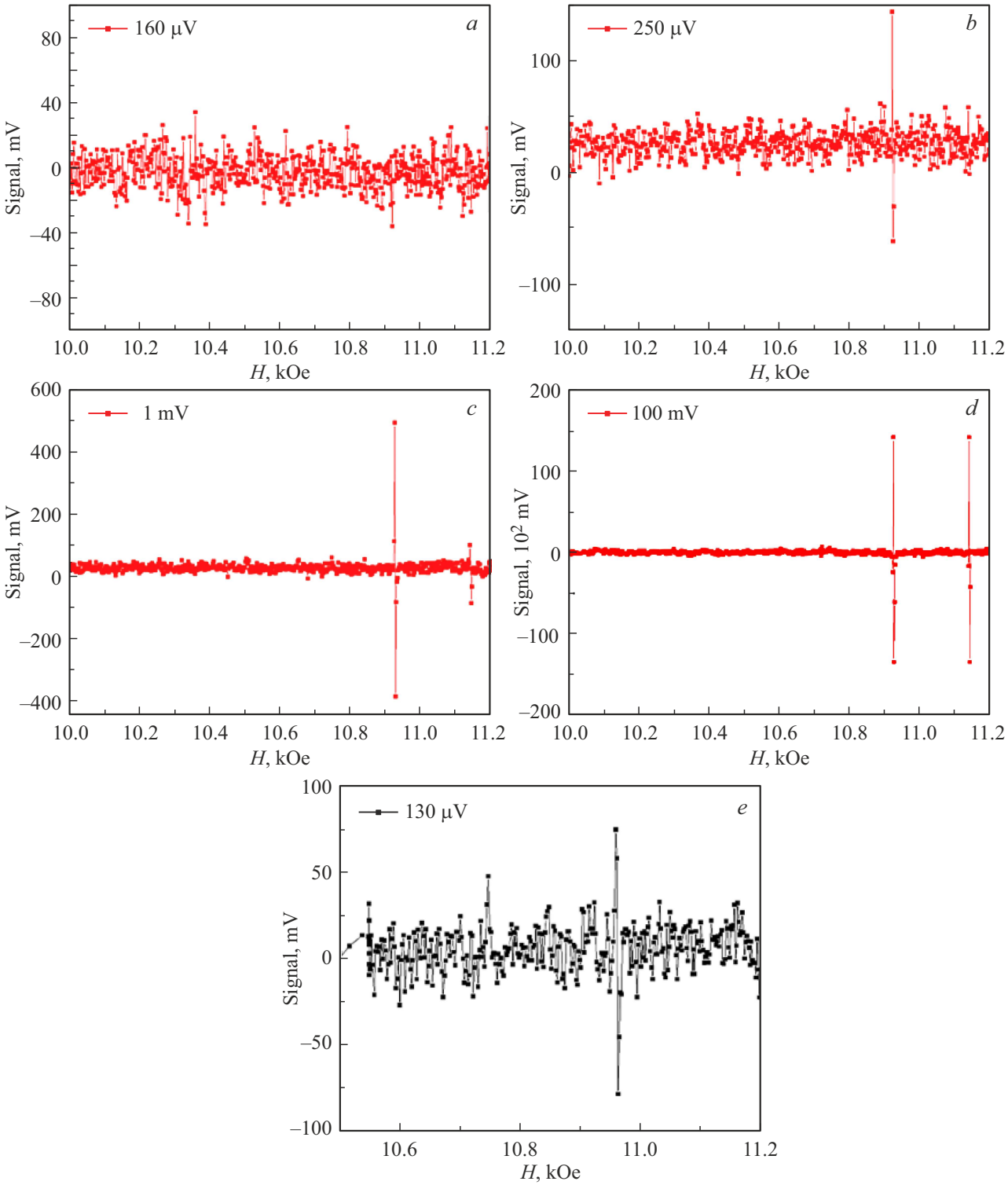

Figure 5. Results of measurements in the waveguide for different configurations and at different microwave power levels: *a*) configuration C, $P_0 = 0.16$ mV; *b*) configuration C, 0.25 mV; *c*) configuration C, 1 mV; *d*) configuration C, 100 mV; *e*) configuration F, 0.13 mV.

5. Conclusion

The obtained set of experimental data allows asserting that CR exists in YIG and manifests itself in magnetic dynamics at sufficiently high microwave frequencies ($\geq$ 30GHz) at room temperature. In some cases, it manifests itself in the form of mixed spin-electron oscillations; in other situations, the coupling between the ferromagnetic spin and electronic subsystems is weakened, and CR can occur in „pure“ form. However, it always

significantly affects the magnetic dynamics of YIG at microwave frequencies. The possibility of CR existence at room temperature can be explained by the fact that electrons inside PSR are shielded from the crystal lattice, as in other quantum wells. In this case, the effective temperature inside PSR is low and phonon scattering is small in case of CR. The electron-electronic relaxation mechanism is also small due to the low concentration ($N \approx 10^{14}\,\mathrm{cm}^{-3}$) of delocalized electrons [2], as well as due to the partial correlation of electron orbits at CR due to the magnetic-dipole coupling of their spins.

Conflict of interest

The authors declare that they have no conflict of interest.

References

[1] B.K. Khannanov, E.I. Golovenchits, V.A. Sanina. JETP Lett. **115**, *4*, 231 (2022).
[2] B. Khannanov, E. Golovenchits, M. Shcheglov, V. Sanina. Nanomater. **13**, *14*, 2147 (2023).
[3] V.G. Bar'yakhtar, V.A. L'vov, D.A. Yablonskii. JETP Lett. **37**, *12*, 673 (1983).
[4] V.A. Fock. Zs. Phys. **47**, *5–8*, 446 (1928).
[5] L.D. Landau. Zs. Phys. **64**, *5*, 629 (1930).
[6] Ya.I. Frenkel, M.P. Bronstein. ZhRFKhO **62**, *5*, 485 (1930). (in Russian).
[7] Y.G. Dorfman. Dokl. AN SSSR **81**, *5*, 765 (1951). (in Russian).
[8] R.B. Dingle. Proc. Royal Soc. London Ser. A Math. Phys. Sci. **212**, *1108*, 94 (1952).
[9] G. Dresselhaus, A.F.K. Kip, C. Kittel. Phys. Rev. **98**, *2*, 368 (1955).
[10] D. Shoenberg. Magnetic oscillations in metals. Cambridge Univ. Press, New York (1984). 570 p.
[11] V.N. Lazukin. UFN **59**, *3*, 553 (1956). (in Russian).
[12] V.V. Romanov, V.A. Kozhevnikov, C.T. Tracey, N.T. Bagraev. Semiconductors **53**, *12*, 1629 (2019).
[13] A.A.Pistolkors, Xu Yan-Shen RiE **5**, *1*, 3 (1960). (in Russian).
[14] Xu Yan-Shen. RiE **5**, *1*, 14 (1960). (in Russian).
[15] A.G. Gurevich, G.A. Melkov. Magnitnye kolebaniya i volny. Fizmatlit, M. (1994). 464 p. (in Russian).

Translated by A.Akhtyamov